

Intracellular Photoactivation of Caspase-3 by Molecular Glues for Spatiotemporal Apoptosis Induction

Nina B. Hentzen,^{†,‡} Rina Mogaki,^{†,‡} Saya Otake,[‡] Kou Okuro,^{*,‡,§} and Takuzo Aida^{*,‡,||}

[†] Laboratorium für Organische Chemie, ETH Zürich, D-CHAB, Vladimir-Prelog-Weg 3, 8093, Zürich, Switzerland

[‡] Department of Chemistry and Biotechnology, School of Engineering, The University of Tokyo, 7-3-1 Hongo, Bunkyo-ku, Tokyo 113-8656, Japan

[§] Department of Chemistry, The University of Hong Kong, Pokfulam Road, Hong Kong, China

^{||} Riken Center for Emergent Matter Science, 2-1 Hirosawa, Wako, Saitama 351-0198, Japan

ABSTRACT: Caspase-3 (Casp-3) is an enzyme that efficiently induces apoptosis, a form of programmed cell death. We report a dendritic molecular glue ^{PC}Glue that enables intracellular delivery of Casp-3 and its photoactivation. ^{PC}Glue carrying multiple guanidinium (Gu⁺) ion pendants via photocleavable linkages can tightly adhere to Casp-3 and deliver it into the cytoplasm mainly by direct penetration through the plasma membrane. Casp-3, whose surface is covered by ^{PC}Glue, is unable to interact with its cellular substrates and can therefore not induce apoptosis. However, upon exposure to UV or two-photon near-infrared (NIR) light, ^{PC}Glue is cleaved off to liberate Casp-3, triggering the apoptotic signaling cascade. This intracellular photoactivation of Casp-3 allows spatiotemporal induction of apoptosis in irradiated cells.

Molecules that induce apoptosis,¹ a process of cell death without releasing harmful substances to the surrounding area, are attractive for cancer therapy.² In the apoptosis signaling cascade, effector caspases such as caspase-3 (Casp-3) are produced as the downstream enzymes that execute the apoptotic process.³ Therefore, intracellular delivery of Casp-3, which allows direct induction of the apoptosis without affecting other non-target signaling pathways, is a promising approach for efficient, low-side-effect cancer therapy.³ For incorporating effector caspases into cancer cells, carriers based on lipids,^{4a} peptides,^{4b} lipid/peptide hybrids,^{4c} carbon nanotubes,^{4d} and gold nanorods,^{4e} have been previously developed. These carriers can deliver active Casp-3 into the cytoplasm, thereby inducing apoptosis.⁴ However, they can also enter non-target cells, leading to serious side effects. Therefore, a particular mechanism for site-selective operation needs to be incorporated into such carriers.

Here we report a dendritic molecular glue ^{PC}Glue (Figure 1) that enables both intracellular delivery and spatiotemporal activation of Casp-3. Previously, we developed water-soluble molecular glues⁵⁻⁹ bearing multiple guanidinium ion (Gu⁺) pendants,¹⁰ which tightly adhere to proteins,⁶ nucleic acids,⁷ phospholipid membranes,⁸ and clay nanosheets⁹ via the formation of multiple salt bridges between their Gu⁺ pendants and oxyanionic groups on the above targets. In 2019, we developed photocleavable molecular glue ^{PC}Glue (Figure 1), which carries nine Gu⁺ pendants via photocleavable linkages (butyrate-substituted nitroveratryloxycarbonyl; ^{BANVOC})¹¹ and a fluorescent nitrobenzoxadiazole (NBD) moiety at the focal core.^{6h} ^{PC}Glue adheres to a growth factor and covers its surface, thereby suppressing the interaction with a receptor protein. Upon UV irradiation, ^{PC}Glue is cleaved off at its ^{BANVOC} linkages (Figure 1) to re-

duce the multivalency for the adhesion and liberates the growth factor for the interaction with the receptor. This successful turning off

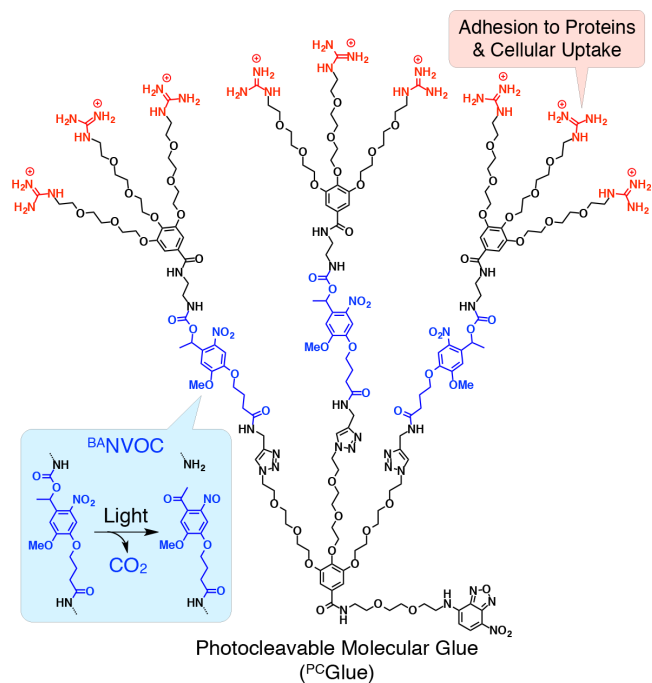


Figure 1. Molecular structure of photocleavable molecular glue ^{PC}Glue, carrying nine Gu⁺ pendants and butyrate-substituted nitroveratryloxycarbonyl (^{BANVOC}) linkages.¹¹ The ^{BANVOC} linkage is cleaved off by exposure to UV or two-photon near-infrared (NIR) light. The focal core of ^{PC}Glue is functionalized with nitrobenzoxadiazole (NBD).

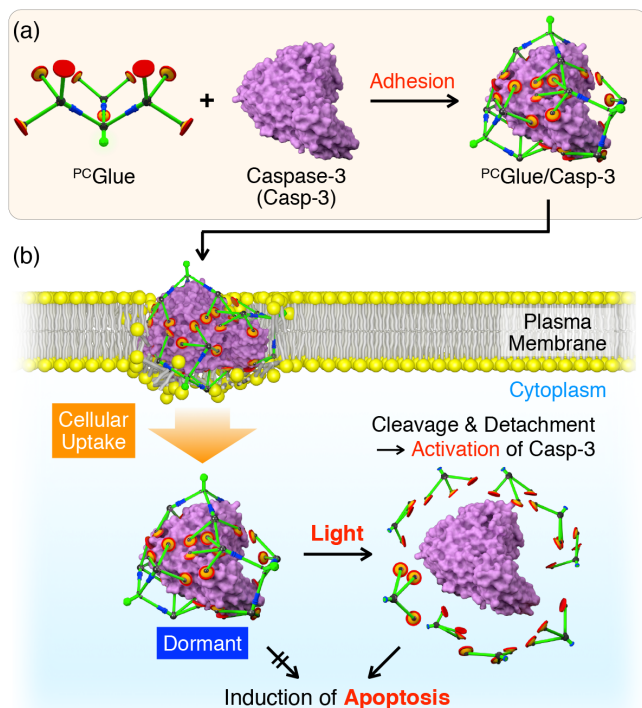


Figure 2. Schematic illustration of apoptosis induction through intracellular photoactivation of caspase-3 (Casp-3) using ^{PC}Glue. (a) ^{PC}Glue adheres to Casp-3, forming their hybrid. (b) The ^{PC}Glue/Casp-3 hybrid enters living cells, presumably by direct penetration through the plasma membrane. Casp-3 covered with ^{PC}Glue is dormant for inducing apoptosis. Upon photoirradiation, ^{PC}Glue on Casp-3 is cleaved off at the photocleavable linkages to reduce the multivalency for the adhesion and consequently liberates Casp-3. Then, the liberated Casp-3 induces the cell apoptosis.

and on the “extracellular” growth factor/receptor interaction prompted us to investigate the possibility of “intracellular” photoactivation of Casp-3 using ^{PC}Glue for spatiotemporal apoptosis induction. A ^{PC}Glue/Casp-3 hybrid (Figure 2a), formed by the adhesion of ^{PC}Glue to Casp-3, supposedly enters living cells¹² by direct penetration through the plasma membrane (Figure 2b), as previously reported for the hybrids of dendritic molecular glues and siRNA.^{7c} Within the cells, Casp-3, whose surface is covered with ^{PC}Glue, is unable to interact with its cellular substrates and therefore inactive for inducing apoptosis (dormant; Figure 2b). In this communication, we report, for the first time, intracellular photoactivation of Casp-3 using ^{PC}Glue (Figure 2b). Spatiotemporal apoptosis induction with the ^{PC}Glue/Casp-3 hybrid by two-photon near-infrared (NIR) light is also highlighted.

We first confirmed the adhesion of ^{PC}Glue to Casp-3. Dynamic light scattering (DLS) analysis in phosphate buffered saline (PBS; 15% glycerol, pH 7.4) indicated that the hydrodynamic diameter (D_h) of Casp-3 (0.4 μ M; $D_h = 0.7 \pm 0.1$ nm; Figure 3a, purple) increased upon addition of ^{PC}Glue (10 μ M; $D_h = 2.5 \pm 0.8$ nm; Figure 3a, green). Accordingly, the zeta potential (ζ) of Casp-3 (0.4 μ M; $\zeta = -9.3$ mV; Figure 3b, purple) became positive ($\zeta = +8.5$ mV; Figure 3b, green) after the addition of ^{PC}Glue (10 μ M). This is most likely due to the charge neutralization of the carboxylate anions on Casp-3 by the salt-bridge formation with Gu^+ on ^{PC}Glue.

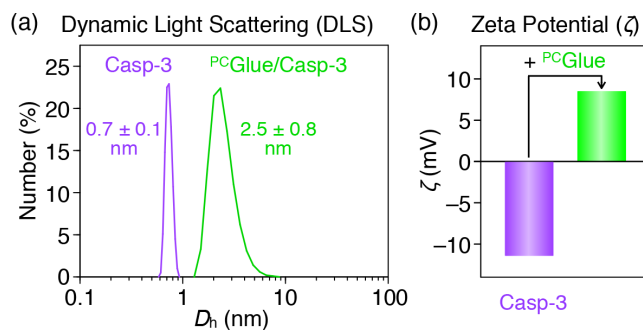


Figure 3. (a) Dynamic light scattering (DLS) histograms at 25 °C in PBS (15% glycerol, pH 7.4) of Casp-3 (0.4 μ M; purple) and a mixture of ^{PC}Glue (10 μ M) and Casp-3 (0.4 μ M; green). (b) Zeta potential (ζ) values at 25 °C in PBS (15% glycerol, pH 7.4) of Casp-3 (0.4 μ M; purple) and a mixture of ^{PC}Glue (10 μ M) and Casp-3 (0.4 μ M; green).

^{PC}Glue efficiently carries Casp-3 into living cells. Here, we used human hepatocellular carcinoma Hep3B cells (1.0×10^4 cells/well), which is a widely used liver cancer cell line, as a model. Hep3B cells were incubated in a serum-free Eagle’s minimal essential medium (EMEM, 200 μ L) containing a mixture of ^{PC}Glue (1 μ M) and Casp-3 (40 nM) for 3 h at 37 °C. After being rinsed with Dulbecco’s phosphate-buffered saline (D-PBS, 200 μ L \times 2), the cell sample was incubated at 37 °C for 30 min in EMEM containing a mixture of 10% fetal bovine serum (FBS) and LysoTracker Red (25 nM) as an endosome-labeling reagent, and then subjected to confocal laser scanning microscopy. Upon excitation at 488 nm, a fluorescence emission assignable to the NBD of ^{PC}Glue was observed from the cell interior (Figure 4a). The fluorescence signals barely overlap with those from LysoTracker Red ($\lambda_{\text{ext}} = 552$ nm, Figures 4b and 4c), suggesting that cellular uptake of the ^{PC}Glue/Casp-3 hybrid occurs mainly by direct penetration through the plasma membrane rather than endocytosis. In fact, Hep3B cells incubated with ^{PC}Glue (1 μ M) and Casp-3 (40 nM) for 1 h at 4 °C, where endocytosis is known to be suppressed,¹³ also emitted fluorescence due to the NBD unit of ^{PC}Glue (Figure S1).¹⁴

Photoirradiation successfully induces apoptosis for the Hep3B cells treated with the ^{PC}Glue/Casp-3 hybrid. The enzymatic activity of intracellular Casp-3 was evaluated by using a commercially available substrate NucView.¹⁵ When cleaved by Casp-3, NucView releases a dye that migrates into the cell nucleus and then emits fluorescence upon excitation at 552 nm.¹⁵ Hep3B cells (1.0×10^4 cells/well) were incubated in EMEM (200 μ L) containing a mixture of ^{PC}Glue (1 μ M) and Casp-3 (40 nM) for 3 h at 37 °C. After rinsing with D-PBS (200 μ L \times 2), the cell sample was supplied with EMEM (10% FBS, 200 μ L) and exposed to UV light ($\lambda = 365$ nm, 1.1 mW/mm²) for 2 min, followed by the addition of NucView (2 μ M). Then, the cell sample was incubated for 18 h at 37 °C and subjected to confocal laser scanning microscopy. As shown in Figures 4e and 4f (red), the cells emitted fluorescence from their nuclei ($\lambda_{\text{ext}} = 552$ nm), indicating the activation of Casp-3 inside the cells. Image analysis of the micrographs revealed that 77% of the cells accommodated active Casp-3 and were namely apoptotic (Table S1; apoptotic rate).^{14,16} Cell viability test using Cell Counting Kit-8 (CCK-8) also suggested the apoptosis of cells (Figure 4g, red). In sharp contrast, a reference cell sample prepared without UV irradiation under otherwise identical conditions was negligibly

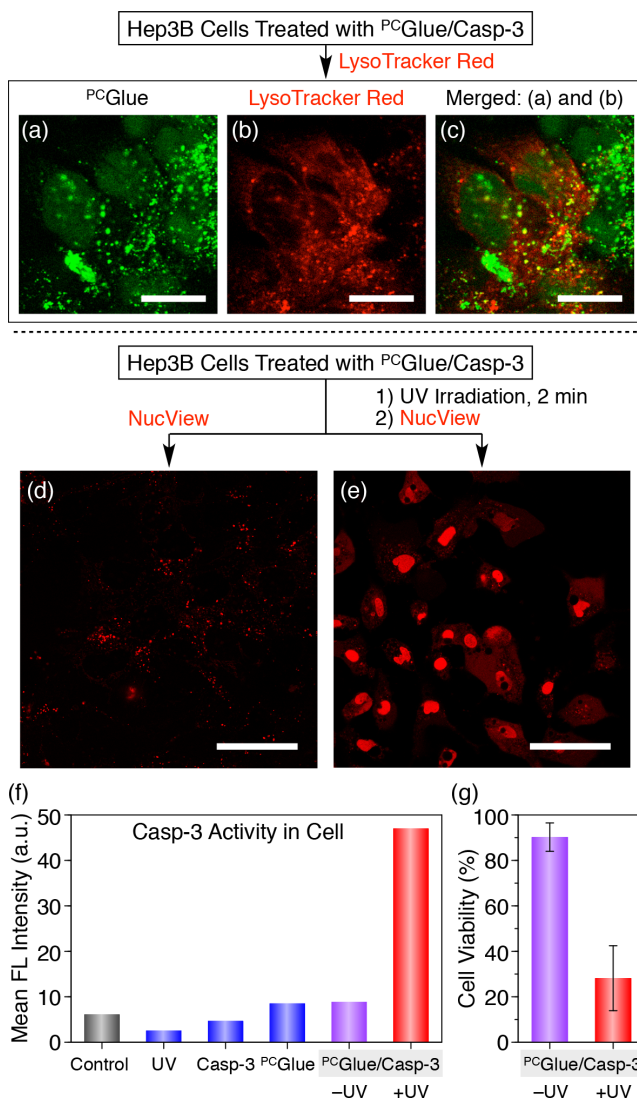


Figure 4. (a–e) Confocal laser scanning micrographs of Hep3B cells after 3 h incubation at 37 °C in EMEM containing ^{PC}Glue (1 μ M) and Casp-3 (40 nM) followed by rinsing with D-PBS. (a, b) Micrographs recorded upon excitation at (a) 488 nm ($\lambda_{\text{obs}} = 500\text{--}530$ nm) and (b) 552 nm ($\lambda_{\text{obs}} = 565\text{--}620$ nm) after 30 min incubation in EMEM (10% FBS) containing LysoTracker Red (25 nM). (c) Merged image of (a) and (b). Scale bars = 20 μ m. (d, e) Micrographs recorded upon excitation at 552 nm ($\lambda_{\text{obs}} = 565\text{--}620$ nm). The Hep3B cells, treated with EMEM containing ^{PC}Glue (1 μ M) and Casp-3 (40 nM), were incubated at 37 °C for 18 h in EMEM (10% FBS) containing NucView (2 μ M) before (d) and after (e) 2 min UV exposure at 365 nm. Scale bars = 50 μ m. (f) Mean fluorescence (FL) intensities of Hep3B cells evaluated from the micrographs (d), (e), and those of Hep3B cells treated with Casp-3 (40 nM) or ^{PC}Glue (1 μ M) as well as untreated cells before and after 2 min UV exposure at 365 nm (Figure S2).¹⁴ (g) Viabilities of Hep3B cells after 12 h incubation at 37 °C in EMEM (10% FBS) containing ^{PC}Glue (1 μ M) and Casp-3 (50 nM) before (purple) and after (red) 2 min UV exposure at 365 nm.

fluorescent upon excitation at 552 nm (Figures 4d and 4f, purple). In fact, cell death was barely induced (Figure 4g, purple). Importantly, neither the UV exposure ($\lambda = 365$ nm, Figure S2b),¹⁴ Casp-3 (40 nM, Figure S2c),¹⁴ nor ^{PC}Glue (1 μ M, Figure S2d)¹⁴

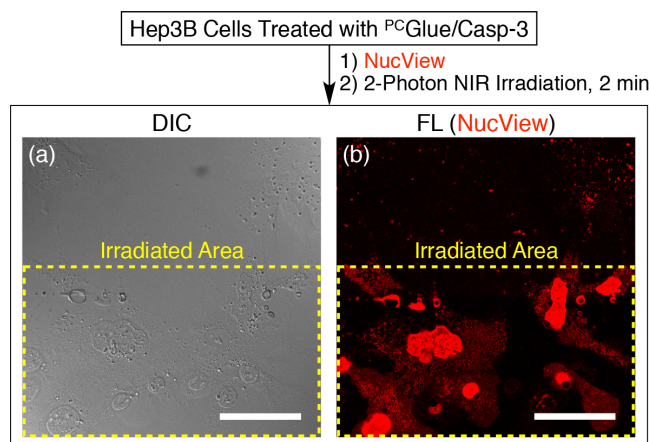


Figure 5. (a) Differential interference contrast (DIC) and (b) confocal laser scanning micrographs upon excitation at 514 nm ($\lambda_{\text{obs}} = 540\text{--}660$ nm) of Hep3B cells. Hep3B cells were incubated at 37 °C for 3 h in EMEM containing a mixture of ^{PC}Glue (1 μ M) and Casp-3 (40 nM), rinsed with D-PBS, and then incubated at 37 °C for 18 h in EMEM (10% FBS) containing NucView (2 μ M), followed by two-photon irradiation at 710 nm for 2 min. The yellow dashed boxes in (a) and (b) represent the irradiated area. Scale bars = 50 μ m.

could activate Hep3B cells for NucView (Figure 4f). Accordingly, none of the reference cell samples were significantly apoptotic (apoptotic rate: 6%–29%, Table S1).¹⁴

Of particular interest, such an intracellular activation of Casp-3 could be achieved in a spatiotemporal manner with two-photon NIR light. This is advantageous for *in vivo* applications because NIR light can penetrate deep tissues.¹⁷ Analogous to the previous experiment (Figure 4d), Hep3B cells were incubated with ^{PC}Glue/Casp-3 ($[\text{PCGlue}] = 1 \mu\text{M}$, $[\text{Casp-3}] = 40 \text{ nM}$) and then treated with NucView (2 μ M). When irradiated with a two-photon NIR laser ($\lambda = 710$ nm; Figures 5 and S4, yellow dashed box)¹⁴ for 2 min, the cells located in the irradiated area exhibited a strong fluorescence in the nuclei due to NucView (Figures 5b and S4b).¹⁴ In sharp contrast, the cells in the nonirradiated area remained non-fluorescent (Figures 5b and S4b).¹⁴ These results indicate that ^{PC}Glue can be cleaved at the ^{BAN}VOC linkages by two-photon NIR light^{8b,18} and successfully liberate active Casp-3 inside cells.

In conclusion, we demonstrated that ^{PC}Glue carries Casp-3 directly into the cytoplasm and liberates it by using UV or two-photon NIR light. Consequently, apoptosis occurs selectively in the irradiated cells. This unprecedented intracellular photoactivation of Casp-3 using NIR light is advantageous for *in vivo* practical applications. Thus, an *in vivo* study on phototherapy of cancer using the ^{PC}Glue/Casp-3 hybrid is a subject worthy of further investigation.

ASSOCIATED CONTENT

Supporting Information

The Supporting Information is available free of charge on the ACS Publications website.

Confocal microscopic images and related experimental procedures (PDF)

AUTHOR INFORMATION

Corresponding Authors

*okuro@hku.hk (K.O.)

*aida@macro.t.u-tokyo.ac.jp (T.A.)

Author Contributions

†N.B.H. and R.M. contributed equally.

Notes

The authors declare no competing financial interest.

ACKNOWLEDGMENTS

This work was supported by JSPS KAKENHI Early-Career Scientists (18K14353) to K.O. and partially supported by Grant-in-Aid for Scientific Research (S) (18H05260) to T.A. We appreciate Prof. H. Cabral (the Univ. of Tokyo) for DLS and zeta-potential measurements. We also thank Leica Microsystems for confocal laser scanning microscopy with a two-photon laser. N.B.H. thanks Japan Society for the Promotion of Science (JSPS) for Young Researchers' Exchange Program between Japan and Switzerland. R.M. and S.O. thank the Research Fellowships of JSPS for Young Scientists.

REFERENCES

- (1) (a) Raff, M. Cell suicide for beginners. *Nature* **1998**, *396*, 119–122. (b) Thornberry, N. A.; Lazebnik, Y. Caspases: enemies within. *Science* **1998**, *281*, 1312–1316. (c) Taylor, R. C.; Cullen, S. P.; Martin, S. J. Apoptosis: controlled demolition at the cellular level. *Nat. Rev. Mol. Cell Biol.* **2008**, *9*, 231–241.
- (2) Reed, J. C. Apoptosis-based therapies. *Nat. Rev. Drug Discovery* **2002**, *1*, 111–121.
- (3) (a) Salvesen, G. S.; Dixit, V. M. Caspases: intracellular signaling by proteolysis. *Cell* **1997**, *91*, 443–446. (b) Budihardjo, I.; Oliver, H.; Lutter, M.; Luo, X.; Wang, X. Biochemical Pathways of Caspase Activation During Apoptosis. *Annu. Rev. Cell Dev. Biol.* **1999**, *15*, 269–290. (c) McArthur, K.; Kile, B. T. Apoptotic Caspases: Multiple or Mistaken Identities? *Trends Cell Biol.* **2018**, *28*, 475–493.
- (4) (a) Zelphati, O.; Wang, Y.; Kitada, S.; Reed, J. C.; Felgner, P. L.; Corbeil, J. Intracellular Delivery of Proteins with a New Lipid-mediated Delivery System. *J. Biol. Chem.* **2001**, *276*, 35103–35110. (b) Fu, J.; Yu, C.; Li, L.; Yao, S. Q. Intracellular Delivery of Functional Proteins and Native Drugs by Cell-Penetrating Poly(disulfide)s. *J. Am. Chem. Soc.* **2015**, *137*, 12153–12160. (c) Tang, R.; Kim, C. S.; Solfield, D. J.; Rana, S.; Mout, R.; Velázquez-Delgado, E. M.; Chompoosor, A.; Jeong, Y.; Yan, B.; Zhu, Z.-J.; Kim, C.; Hardy, J. A.; Rotello, V. M. Direct Delivery of Functional Proteins and Enzymes to the Cytosol Using Nanoparticle-Stabilized Nanocapsules. *ACS Nano* **2013**, *7*, 6667–6673. (d) Cheng, Q.; Blais, M.-O.; Harris, G.; Jabbarzadeh, E. PLGA-Carbon Nanotube Conjugates for Intercellular Delivery of Caspase-3 into Osteosarcoma Cells. *PLoS One* **2013**, *8*, e81947. (e) Esteban-Fernández de Ávila, B.; Ramírez-Herrera, D. E.; Campuzano, S.; Angsantikul, P.; Zhang, L.; Wang, J. Nanomotor-Enabled pH-Responsive Intracellular Delivery of Caspase-3: Toward Rapid Cell Apoptosis. *ACS Nano* **2017**, *11*, 5367–5374.
- (5) Mogaki, R.; Hashim, P. K.; Okuro, K.; Aida, T. Guanidinium-based “molecular glues” for modulation of biomolecular functions. *Chem. Soc. Rev.* **2017**, *46*, 6480–6491.
- (6) (a) Okuro, K.; Kinbara, K.; Tsumoto, K.; Ishii, N.; Aida, T. Molecular Glues Carrying Multiple Guanidinium Ion Pendants via an Oligoether Spacer: Stabilization of Microtubules against Depolymerization. *J. Am. Chem. Soc.* **2009**, *131*, 1626–1627. (b) Okuro, K.; Kinbara, K.; Takeda, K.; Inoue, Y.; Ishijima, A.; Aida, T. Adhesion Effects of a Guanidinium Ion Appended Dendritic “Molecular Glue” on the ATP-Driven Sliding Motion of Actomyosin. *Angew. Chem., Int. Ed.* **2010**, *49*, 3030–3033. (c) Uchida, N.; Okuro, K.; Niitani, Y.; Ling, X.; Ariga, T.; Tomishige, M.; Aida, T. Photoclickable Dendritic Molecular Glue: Noncovalent-to-Covalent Photochemical Transformation of Protein Hybrids. *J. Am. Chem. Soc.* **2013**, *135*, 4684–4687. (d) Garzoni, M.; Okuro, K.; Ishii, N.; Aida, T.; Pavan, G. M. Structure and Shape Effects of Molecular Glue on Supramolecular Tubulin Assemblies. *ACS Nano* **2014**, *8*, 904–914. (e) Mogaki, R.; Okuro, K.; Aida, T. Molecular glues for manipulating enzymes: trypsin inhibition by benzamidinium-conjugated molecular glues. *Chem. Sci.* **2015**, *6*, 2802–2805. (f) Okuro, K.; Sasaki, M.; Aida, T. Boronic Acid-Appended Molecular Glues for ATP-Responsive Activity Modulation of Enzymes. *J. Am. Chem. Soc.* **2016**, *138*, 5527–5530. (g) Mogaki, R.; Okuro, K.; Aida, T. Adhesive Photoswitch: Selective Photochemical Modulation of Enzymes under Physiological Conditions. *J. Am. Chem. Soc.* **2017**, *139*, 10072–10078. (h) Mogaki, R.; Okuro, K.; Ueki, R.; Sando, S.; Aida, T. Molecular Glue that Spatiotemporally Turns on Protein–Protein Interactions. *J. Am. Chem. Soc.* **2019**, *141*, 8035–8040.
- (7) (a) Hashim, P. K.; Okuro, K.; Sasaki, S.; Hoashi, Y.; Aida, T. Reductively Cleavable Nanocaplets for siRNA Delivery by Template-Assisted Oxidative Polymerization. *J. Am. Chem. Soc.* **2015**, *137*, 15608–15611. (b) Hatano, J.; Okuro, K.; Aida, T. Photoinduced Bioorthogonal 1,3-Dipolar Poly-cycloaddition Promoted by Oxyanionic Substrates for Spatiotemporal Operation of Molecular Glues. *Angew. Chem., Int. Ed.* **2016**, *55*, 193–198. (c) Okuro, K.; Nemoto, H.; Mogaki, R.; Aida, T. Dendritic Molecular Glues with Reductively Cleavable Guanidinium Ion Pendants: Highly Efficient Intracellular siRNA Delivery via Direct Translocation. *Chem. Lett.* **2018**, *47*, 1232–1235. (d) Kohata, A.; Hashim, P. K.; Okuro, K.; Aida, T. Transferrin-Appended Nanocaplet for Transcellular siRNA Delivery into Deep Tissues. *J. Am. Chem. Soc.* **2019**, *141*, 2862–2866.
- (8) (a) Suzuki, Y.; Okuro, K.; Takeuchi, T.; Aida, T. Friction-Mediated Dynamic Disordering of Phospholipid Membrane by Mechanical Motions of Photoresponsive Molecular Glue: Activation of Ion Permeation. *J. Am. Chem. Soc.* **2012**, *134*, 15273–15276. (b) Arisaka, A.; Mogaki, R.; Okuro, K.; Aida, T. Caged Molecular Glues as Photoactivatable Tags for Nuclear Translocation of Guests in Living Cells. *J. Am. Chem. Soc.* **2018**, *140*, 2687–2692.
- (9) (a) Wang, Q.; Mynar, J. L.; Yoshida, M.; Lee, E.; Lee, M.; Okuro, K.; Kinbara, K.; Aida, T. High-water-content mouldable hydrogels by mixing clay and a dendritic molecular binder. *Nature* **2010**, *463*, 339–343. (b) Tamesue, S.; Ohtani, M.; Yamada, K.; Ishida, Y.; Spruell, J. M.; Lynd, N. A.; Hawker, C. J.; Aida, T. Linear versus Dendritic Molecular Binders for Hydrogel Network Formation with Clay Nanosheets: Studies with ABA Triblock Copolyethers Carrying Guanidinium Ion Pendants. *J. Am. Chem. Soc.* **2013**, *135*, 15650–15655.
- (10) (a) Sakai, N.; Matile, S. Anion-Mediated Transfer of Polyarginine across Liquid Bilayer Membranes. *J. Am. Chem. Soc.* **2003**, *125*, 14348–14356. (b) Hennig, A.; Gabriel, G. J.; Tew, G. N.; Matile, S. Stimuli-Responsive Polyguanidino-Oxanorbornene Membrane Transporters as Multicomponent Sensors in Complex Matrices. *J. Am. Chem. Soc.* **2008**, *130*, 10338–10344. (c) Shukla, D.; Schneider, C. P.; Trout, B. L. Complex Interactions between Molecular Ions in Solution and Their Effect on Protein Stability. *J. Am. Chem. Soc.* **2011**, *133*, 18713–18718. (d) Geihe, E. I.; Cooley, C. B.; Simon, J. R.; Kiesewetter, M. K.; Edward, J. A.; Hickerson, R. P.; Kaspar, R. L.; Hedrick, J. L.; Waymouth, R. M.; Wender, P. A. Designed guanidinium-rich amphipathic oligocarbonate molecular transporters complex, deliver and release siRNA in cells. *Proc. Natl. Acad. Sci. U. S. A.* **2012**, *109*, 13171–13176. (e) Bang, E.-K.; Gasparini, G.; Molinard, G.; Roux, A.; Sakai, N.; Matile, S. Substrate-Initiated Synthesis of Cell-Penetrating Poly(disulfide)s. *J. Am. Chem. Soc.* **2013**, *135*, 2088–2091. (f) Gasparini, G.; Bang, E.-K.; Molinard, G.; Tulumello, D. V.; Ward, S.; Kelley, S. O.; Roux, A.; Sakai, N.; Matile, S. Cellular Uptake of Substrate-Initiated Cell-Penetrating Poly(disulfide)s. *J. Am. Chem. Soc.* **2014**, *136*, 6069–6074. (g) Gasparini, G.; Matile, S. Protein delivery with cell-penetrating poly(disulfide)s. *Chem. Commun.* **2015**, *51*, 17160–17162. (h) McKinlay, C. J.; Waymouth, R. M.; Wender, P. A. Cell-Penetrating, Guanidinium-Rich Oligophosphoesters: Effective and Versatile Molecular Transporters for Drug and Probe Delivery. *J. Am. Chem. Soc.* **2016**, *138*, 3510–3517. (i) Derivery, E.; Bartolami, E.; Matile, S.; Gonzalez-Gaitan, M. Efficient Delivery of Quantum Dots into the Cytosol of Cells Using Cell-Penetrating Poly(disulfide)s. *J. Am. Chem. Soc.* **2017**, *139*, 10172–10175.
- (11) (a) Klán, P.; Šolomek, T.; Bochet, C. G.; Blanc, A.; Givens, R.; Rubina, M.; Popik, V.; Kostikov, A.; Wirz, J. Photoremovable Protecting Groups in Chemistry and Biology: Reaction Mechanisms and Efficacy. *Chem. Rev.* **2013**, *113*, 119–191. (b) Hansen, M. J.; Velema, W. A.; Lerch, M.

M.; Szymanski, W.; Feringa, B. L. Wavelength-selective cleavage of photoprotecting groups: strategies and applications in dynamic systems. *Chem. Soc. Rev.* **2015**, *44*, 3358–3377.

(12) (a) Nischan, N.; Herce, H. D.; Natale, F.; Bohlke, N.; Budisa, N.; Cardoso, M. C.; Hackenberger, C. P. R. Covalent Attachment of Cyclic TAT Peptides to GFP Results in Protein Delivery into Live Cells with Immediate Bioavailability. *Angew. Chem., Int. Ed.* **2015**, *54*, 1950–1953. (b) Nagel, Y. A.; Raschle, P. S.; Wennemers, H. Effect of Preorganized Charge-Display on the Cell-Penetrating Properties of Cationic Peptides. *Angew. Chem., Int. Ed.* **2017**, *56*, 122–126. (c) Schneider, A. F. L.; Wallabregue, A. L. D.; Franz, L.; Hackenberger, C. P. R. Targeted Subcellular Protein Delivery Using Cleavable Cyclic Cell-Penetrating Peptides. *Bioconjugate Chem.* **2019**, *30*, 400–404.

(13) Casley-Smith, J. R. Endocytosis: The Different Energy Requirements for the Uptake of Particles by Small and Large Vesicles into Peritoneal Macrophages. *J. Microsc.* **1969**, *90*, 15.

(14) See Supporting Information.

(15) (a) Manas, A.; Wang, S.; Nelson, A.; Li, J.; Zhao, Y.; Zhang, H.; Davis, A.; Xie, B.; Maltsev, N.; Xiang, J. The Functional Domains for Bax2 Aggregate-mediated Caspase 8-Dependent Cell Death. *Exp. Cell Res.* **2017**, *359*,

342–355. (b) Bueno, O.; Gallego, J. E.; Martins, S.; Prota, A. E.; Gago, F.; Gómez-SanJuan, A.; Camarasa, M.-J.; Barasoain, I.; Steinmetz, M. O.; Díaz J. F.; Pérez-Pérez, M.-J.; Liekens, S.; Priego, E.-M. High-Affinity Ligands of the Colchicine Domain in Tubulin Based on a Structure-guided Design. *Sci. Rep.* **2018**, *8*, 4242.

(16) Prieto, A.; Diaz, D.; Barcenilla, H.; Garcia-Suárez, J.; Eduardo, R.; Monserrat, J.; Antonio, E. S.; Melero, D.; de la Hera, A.; Orfao, A.; Alvarez-Mon, M. Apoptotic Rate: A New Indicator for the Quantification of the Incidence of Apoptosis in Cell Cultures. *Cytometry, Part A* **2002**, *48*, 185–193.

(17) Shanmugam, V.; Selvakumar, S.; Yeh, C.-S. Near-Infrared Light-responsive Nanomaterials in Cancer Therapeutics. *Chem. Soc. Rev.* **2014**, *43*, 6254–6287.

(18) Furuta, T.; Wang, S. S.-H.; Dantzker, J. L.; Dore, T. M.; Bybee, W. J.; Callaway, E. M.; Denk, W.; Tsien, R. Y. Brominated 7-Hydroxycoumarin-4-ylmethyls: Photolabile Protecting Groups with Biologically Useful Cross-Sections for Two Photon Photolysis. *Proc. Natl. Acad. Sci. U. S. A.* **1999**, *96*, 1193–1200.

For Table of Contents Only

